

COMMUNICATION

and downfield, respectively, and for cage **2** the previously sharp CH₂ bridge singlet of L2 at 5.19 ppm becomes a complex multiplet as free rotation is hindered (Fig. S15). ROESY spectra of **1** and **2** give expected couplings, including between H_{H'} on the ppy's and the *ortho* pyridyl protons of L (Figs. S8, S16). Diffusion ordered NMR in *d*₃-MeNO₂ for **1**·3PF₆ (Fig. S9) gave a hydrodynamic radius of 18.99 Å.

The structure of **1**·3BF₄·*n*(MeNO₂) was confirmed by crystallography, Fig. 1.^[9] There are two independent cage **1** cations that show minor structural differences. Anions and additional solvent were not located due to significant disorder. Each cage has three pseudo-octahedrally coordinated Ir(III) centers, each with two ppy ligands and the pyridyl groups from two L1 ligands in a *cis* arrangement. The two L1 ligands bridge between three Ir(III) centers. Average torsion angle between *cis* pyridyl groups is 38.04°, typical for [Ir(ppy)₂(pyridyl)₂]-type complexes^[10] with the bowl shape of CTV-type ligands able to accommodate these torsion angles within the cage structure.

Both L1 ligands within each cage **1** are the same enantiomer, giving the chiral *anti*-cryptophane isomer. Each [Ir(ppy)₂]⁺ unit within a cage has the same chirality, such that only the enantiomeric *MM*- $\Lambda\Lambda\Lambda$ and *PP*- $\Delta\Delta\Delta$ cage isomers are observed in the structure. Given the Λ and Δ enantiomers of the [Ir(ppy)₂]⁺ moieties and the *M* and *P* enantiomers of the L-types ligands are present in the reaction mixture, there are twelve possible stereoisomers of the cage.

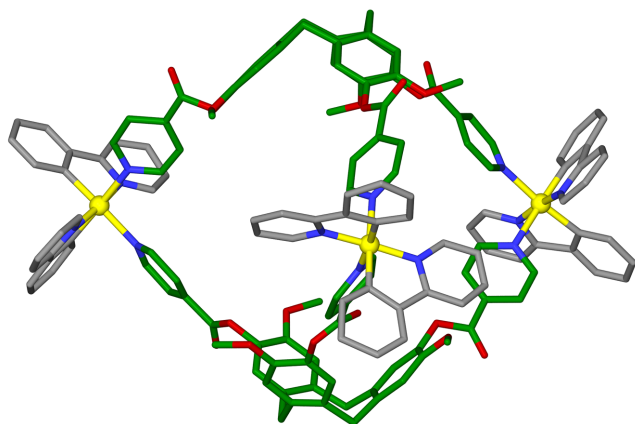


Figure 1. A $\{[Ir(ppy)_2(L1)_2]^{3+}\}$ cage from the crystal structure of **1**·3BF₄·*n*(CH₃NO₂), L1 and ppy ligands shown in green and grey respectively.

The ¹H NMR spectra of both cages **1** and **2** undergo significant sharpening upon standing (Figs. S7 and S15), and fully equilibrate after several months. The ¹H NMR spectrum of cage **1**·3PF₆ collected after 3 months of standing is virtually identical to that of the single crystals of **1**·3BF₄·*n*(CH₃NO₂) re-dissolved in *d*₃-MeNO₂, Fig. 2a/b. (±)-L1 was resolved into its constituent enantiomers by chiral HPLC,^[11] and each L1 enantiomer reacted with each of Λ -[Ir(ppy)₂(MeCN)₂]-BF₄ and Δ -[Ir(ppy)₂(MeCN)₂]-BF₄. As expected, two combinations were mis-matched pairs of enantiomers that gave poorly resolved ¹H NMR spectra (Figs. S10-11) while two combinations were matched pairs (presumably *M*- Δ and *P*- Λ) gave sharp spectra in short timeframes that were similar to the fully sorted cage mixture (Figs. 2d, S12-13). ESI-MS of matched and mis-matched pairs are similar with all combinations showing cage formation (Fig. S14). The observed ¹H NMR spectral sharpening is therefore indicative of equilibration

involving chiral self-sorting of an initial mixture of cage stereoisomers, as was also seen in our previous studies of a [Pd₆(L1)₆]¹²⁺ cage but where only the ligand was a chiral component.^[12] We could not resolve the sorted cages by analytical chiral HPLC.

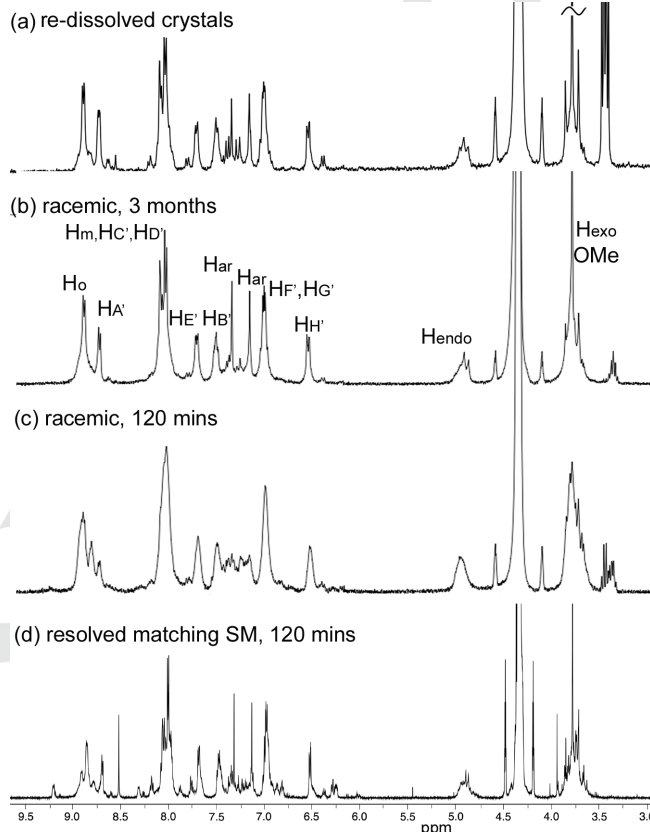


Figure 2. ¹H NMR spectra of cage **1** in CD₃NO₂ of (a) re-dissolved racemic single crystals of *MM*- $\Lambda\Lambda\Lambda$ and *PP*- $\Delta\Delta\Delta$ cages of **1**·3BF₄; (b) (Λ , Δ)-[Ir(ppy)₂(MeCN)₂]-PF₆ and (±)-L1 3 months after mixing; (c) (Λ , Δ)-[Ir(ppy)₂(MeCN)₂]-PF₆ and (±)-L1 two hours after mixing; (d) matched pair of Δ -[Ir(ppy)₂(MeCN)₂]⁺ and one L1 enantiomer after 2 hrs.

Homochiral metallo-cages with *tris*-chelate metal coordination are known both from achiral^[13a-b] and resolved chiral ligands.^[13c-e] Metallo-cages that show homochiral self-sorting from a racemic mixture of ligand enantiomers observed in solution are rare,^[14] though include Pd(II) metallo-cryptophanes.^[8a] The simultaneous chiral self-sorting of both ligand and pre-formed inert metallo-tecton as reported here has not been previously reported.

In a preliminary investigation of the influence of chiral guests on the self-assembly of cage **1** globular additives were included in 3:2 mixtures of (Λ , Δ)-[Ir(ppy)₂(MeCN)₂]-PF₆ and (±)-L1. Addition of chiral *R*-camphor or *S*-camphor led to noticeably faster sharpening of the ¹H NMR spectra than in their absence, but this was not observed for addition of achiral adamantane (Fig. S15-S20). Interestingly, addition of the related anionic species *R*-(or *S*)-10-camphorsulfonic acid to the reaction mixture prevents cage formation presumably as carboxylate is a competing ligand for the iridium (Fig. S21-22).

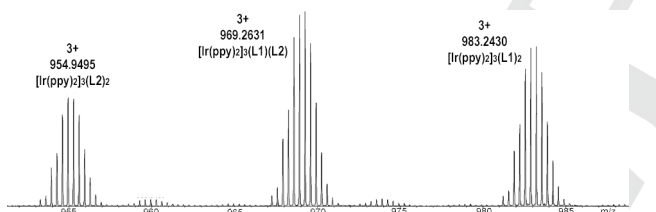
The cages do not show self-recognition of L-ligand species. ESI-MS of a MeNO₂ solution of L1, L2 and [Ir(ppy)₂(MeCN)₂]-BF₄

Table 1. Photophysical properties of complexes **1**·3(BF₄) and **2**·3(BF₄).

| | λ_{em} (nm) | | | Φ_{PL} (%) ^[d] | | | τ_e (ns) ^[g] | | |
|----------|--|--|--------|--------------------------------|---------------|-------------------|-------------------------------|--------------------------------|--------------------------------|
| | DCM (a,b,j) | film (c,f) | powder | DCM (a) | Film (c,f) | powd er (e) | DCM (a) | film (c) | powder |
| 1 | 604 | 481 (0.7), 514 (1), 556 (0.8) | 648 | 1 | 5.5 | 1.3 | 59 (0.7), 129 (0.3) | 634 (0.4), 2319 (0.6) | 55 (0.6), 203 (0.4) |
| 2 | 485 (0.8), 516 (1), 547 (0.6) | 486 (0.8), 515 (1), 545 (0.6) | 519 | 15 | 10 | 1.6 | 523 (0.4), 887 (0.6) | 688 (0.7), 3042 (0.3) | 141 (0.4), 1175 (0.6) |

[a] Measurements in degassed DCM at 298 K. [b] Quinine sulfate employed as the external reference ($\Phi_{PL} = 54.6\%$ in 0.5 M H₂SO₄ at 298 K). [c] PMMA doped films (5 wt % of cage) formed by spin-coating deposition on quartz substrate. [d] Φ_{PL} measurements were carried out under nitrogen ($\lambda_{exc} = 360$ nm). [e] values obtained using an integrating sphere. [f] Principal emission peaks listed with values in brackets indicating relative intensity. [g] $\lambda_{exc} = 378$ nm; Values in parentheses are pre-exponential weighting factor, in relative % intensity, of the emission decay kinetics.

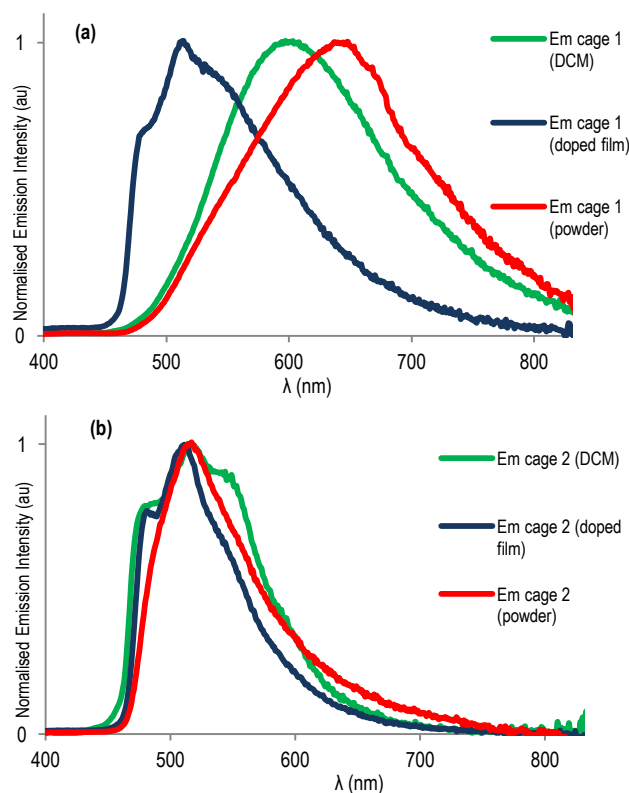
shows a statistical mixture of **1**:{[Ir(ppy)₂]₃(L1)(L2)}³⁺:**2** cage species, Fig. 3. Mixing **1**·3BF₄ and **2**·3BF₄ in MeNO₂ results in very slow exchange between L1 and L2 with appreciable ligand exchange only observed after 4 weeks, and near-statistical mixing reached after 10 weeks (Figure S6). Thus these cages have a high degree of kinetic stability but are not completely inert. It is interesting to note that this speciation behavior is in contrast with recently reported [Pd₃L₂]⁶⁺ metallo-cryptophanes, which exclusively formed homocages from two different L-type ligands, with no ligand exchange.^[8a]

**Figure 3.** ESI-MS of a 1:1:3 mixture of L1:L2: [Ir(ppy)₂(MeCN)₂]⁺·BF₄ in MeNO₂ showing formation of statistical mixture of homoleptic and heteroleptic cages.

The absorption spectra of **1** and **2** in dichloromethane (DCM) are similar to other [Ir(ppy)₂(NⁿN)]⁺ systems,^[7] and characterised by two intense ligand centered (¹LC) transitions between 260 and 320 nm localised on the ppy and three lower intensity broad bands at below 380 nm that consist of spin-allowed and spin-forbidden mixed metal-to-ligand and ligand-to-ligand charge transfer (¹MLCT/¹LLCT and ³MLCT/³LLCT) transitions (Fig. S26). The weak CT transition observed for **1** at 470 nm was not reported for the monomeric [Ir(ppy)₂(4-pyCO₂Et)₂]⁺ (4-pyCO₂Et = 4-ethyl isonicotinate),^[10c] pointing to increased conjugation in **1** due to the CTV scaffold. For both **1** and **2**, the excitation spectra in DCM match the absorption spectra and indicate a single photophysically-active species.

Cages **1** and **2** are emissive in DCM solution and in the solid state. Upon photoexcitation of **1**, a broad and unstructured emission is observed both in DCM and in the powder, Fig. 4a, due to emission from a mixed ³MLCT/³LLCT state.^[7] The photoluminescence spectrum in the powder is red-shifted ($\lambda_{max} = 648$ nm) compared to that in DCM ($\lambda_{max} = 604$ nm); however, **1** possesses similarly low Φ_{PL} of around 1% and bi-exponential decay kinetics in both media, Table 1. Due to the increased conjugation into the CTV scaffold, cage **1** shows red-shifted emission and similar Φ_{PL} compared to [Ir(ppy)₂(4-pyCO₂Et)₂]⁺ ($\lambda_{max} = 560$ nm; $\Phi_{PL} = 2\%$).^[10c] Lusby's {[Ir(ppy)₂]₃(tcb)₄}⁶⁺ cage also showed red-shifted emission ($\lambda_{max} = 575$ nm) when compared with the corresponding [Ir(ppy)₂(NCPH)₂]OTf complex ($\lambda_{max} = 525$ nm); however, unlike for cage **1** and other Ir(ppy)₂ discrete supramolecular systems,^[15] the Φ_{PL} for the Lusby cage was enhanced compared with that of the mononuclear complex ($\Phi_{PL} = 4\%$ cf. $\Phi_{PL} < 1\%$).^[4]

In order to mitigate non-radiative vibrational motion in the cage we spin-coated 5 wt % of **1** in polymethyl methacrylate (PMMA), which serves as an inert matrix. The emission in the thin film was blue-shifted and more structured ($\lambda_{max} = 514$ nm) compared to both the powder and solution spectra. The Φ_{PL} of 5.5% was enhanced as a result of the rigidification conferred by the PMMA host and the emission lifetimes were significantly longer ($\tau_e = 634$ and 2319 ns).

**Figure 4.** Normalised photoluminescence spectra of a) **1**·3BF₄ and b) **2**·3BF₄. Dotted lines de-aerated DCM solution; dashed lines PMMA doped films with 5 wt % of cages spin-coated on a quartz substrate; red lines bulk powders.

The photoluminescence spectrum of cage **2** in DCM is more structured and blue-shifted ($\lambda_{\text{max}} = 516$ nm) compared to **1**, indicating emission that is more predominantly ligand-centered (^3LC) (Fig. 4(b)). The blue-shifted emission of **2** compared to **1** was expected considering the presence of the electron-withdrawing ester moieties located on L1 in **1**, which stabilise the LUMO.^[10c] Cage **2** shows a significantly enhanced Φ_{PL} and longer τ_e compared to **1** in DCM ($\Phi_{\text{PL}} = 15\%$, $\tau_e = 523, 887$ ns).

Unlike for **1**, as a powder the emission of **2** is not significantly red-shifted ($\lambda_{\text{max}} = 519$ nm) though the emission profile is less structured, showing less well-resolved vibrational bands as shoulders of the main emission peak. The emission profile for **2** in PMMA doped thin film is likewise very similar to that in DCM. Though Φ_{PL} values are low in the powder ($\Phi_{\text{PL}} = 1.6\%$), in doped film they are higher ($\Phi_{\text{PL}} = 10\%$). Emission lifetimes are expectedly longer in doped films than in powder, Table 1. Attempts to synthesize an analogous mononuclear complex of 4-phenoxymethylpyridine for comparison were not successful due to ligand oligomerization.

In summary, phosphorescent $[\{\text{Ir}(\text{ppy})_2\}_3(\text{L})_2]^{3+}$ metallo-cryptophanes can be synthesized in high yields, with the CTV-type ligands able to accommodate torsion angles typical of $[\text{Ir}(\text{ppy})_2(\text{L})_2]$ complexes to form rare examples of 3-D Ir(III) cyclometallated coordination cages. These cages undergo ligand exchange processes over months, and show a remarkably high degree of homochiral self-sorting of both ligand and metallo-technon, but not self-recognition between similar L-type ligands. Chiral sorting is enhanced by the presence of neutral chiral additives. For cage **1** chiral self-sorting occurs relatively rapidly upon crystallization through an induced seeding effect, but on a timescale of months in solution. Luminescence properties of the two cages are quite distinct, pointing to an ability to tune the photophysical properties of these systems. Cage **2** showed an enhanced and blue-shifted emission compared to **1**, reaching a Φ_{PL} of 15% in DCM solution and 10% in doped film. These are promising systems for a variety of applications: as semiochemical hosts, photoredox catalysts and in energy conversion materials.

Acknowledgements

We thank the EPSRC (DTG award 1238852, EP/K039202/1, EP/M02105X/1, EP/J001325/1), Leverhulme Trust (RPG-2014-148), University of St Andrews, and the MEXT/JSPS Grants in Aid for Scientific Research (JP25102005 and JP25102001) for funding; Simon Barrett for assistance with NMR; Martin Huscroft for assistance with HPLC, and Stephen Boyer for elemental analysis measurements.

Data accessibility. Data supporting this work can be accessed at DOI:#####.

Keywords: supramolecular chemistry; cage compounds • homochiral self-sorting • phosphorescence

- [1] Reviews: a) S. Zarra, D. M. Wood, D. A. Roberts, J. R. Nitschke, *Chem. Soc. Rev.* **2015**, *44*, 419-432; b) T. R. Cook, Y.-R. Zheng, P. J. Stang, *Chem. Rev.* **2013**, *113*, 734-777; c) K. Harris, M. Fujita, *Chem. Commun.* **2013**, *49*, 6703-6712; d) M. D. Ward, *Chem. Commun.* **2009**, 4487-4499; e) D. Fiedler, D. H. Leung, R. G. Bergman, K. N. Raymond, *Acc. Chem. Res.*, **2005**, *38*, 349-358.
- [2] For examples and reviews a) J. R. Piper, L. Cletheroe, C. G. P. Taylor, A. J. Metherell, J. A. Weinstein, I. V. Sazanovich, M. D. Ward, *Chem. Commun.* **2017**, *53*, 408-411; b) A. Schmidt, M. Hollering, M. Drees, A. Casini, F. E. Kühn, *Dalton Trans.* **2016**, *45*, 8556-8565; c) L. Xu, Y.-X. Wang, H.-B. Yang, *Dalton Trans.* **2015**, *44*, 867-890; d) X. Yan, T. R. Cook, P. Wang, F. Huang, P. J. Stang, *Nature Chem.* **2015**, *7*, 342-348; e) J. E. M. Lewis, A. B. S. Elliot, C. J. McAdam, K. C. Gordon, J. D. Crowley, *Chem. Sci.* **2014**, *5*, 1833-1843; f) Z. Li, N. Kishi, K. Yoza, M. Akita, M. M. Yoshizawa, *Chem. Eur. J.* **2012**, *18*, 8358-8365; g) K. Harano, S. Hiraoka, M. Shionoya, *J. Am. Chem. Soc.* **2007**, *129*, 5300-5301; h) N. K. Al-Rasbi, C. Sabatini, F. Barigelletti, M. D. Ward, *Dalton Trans.* **2006**, 4769-4772.
- [3] A. Schmidt, M. Hollering, J. Han, A. Casini, F. E. Kühn, *Dalton Trans.* **2016**, *45*, 12297-12300; b) A. B. S. Elliot, J. E. M. Lewis, H. van der Salm, C. J. McAdams, J. D. Crowley, K. C. Gordon, *Inorg. Chem.* **2016**, *55*, 3440-3447; c) W. J. Ramsay, J. A. Foster, K. L. Moore, T. K. Ronson, R. J. Mirgalet, D. A. Jefferson, J. R. Nitschke, *Chem. Sci.* **2015**, *6*, 7326-7331.
- [4] O. Chepelin, J. Ujma, X. Wu, A. M. Z. Slawin, M. B. Pitak, S. J. Coles, J. Michel, A. C. Jones, P. E. Barran, P. J. Lusby, *J. Am. Chem. Soc.* **2012**, *134*, 19334-19337.
- [5] a) X. Li, J. Wu, L. Chen, X. Zhong, C. Heng, R. Zhang, C. Duan, *Chem. Commun.* **2016**, *52*, 9628-9631; b) X. Li, J. Wu, C. Heng, R. Zhang, C. Duan, *Chem. Commun.* **2016**, *52*, 5104-5107.
- [6] a) C. Shen, A. D. W. Kennedy, W. A. Donald, A. M. Torres, W. S. Price, J. E. Beves, *Inorg. Chim. Acta.* **2017**, *458*, 122-128; b) J. Yang, M. Bhadbhade, W. A. Donald, H. Iranmanesh, E. G. Moore, H. Yan, J. E. Beves, *Chem. Commun.* **2015**, *51*, 4465-4468; c) A. B. Wragg, A. J. Metherell, W. Cullen and M. D. Ward, *Dalton Trans.* **2015**, *44*, 17939-17949; d) K. Li, L.-Y. Zhang, C. Yan, S.-C. Wei, M. Pan, L. Zhang, C.-Y. Su, *J. Am. Chem. Soc.* **2014**, *136*, 4456-4459.
- [7] a) D. R. Martir, A. K. Bansal, V. Di Mascio, D. B. Cordes, A. F. Henwood, A. M. Z. Slawin, P. C. J. Kamer, L. Martinez-Sarti, A. Pertegás, H. J. Bolink, I. D. W. Samuel, E. Zysman-Colman, *Inorg. Chem. Front.* **2016**, *3*, 218-235; b) A. M. Bünzli, E. C. Constable, C. E. Housecroft, A. Prescimone, J. A. Zampese, G. Longo, L. Gil-Escrig, A. Pertegás, E. Ortí, H. J. Bolink, *Chem. Sci.* **2015**, *6*, 2843-2852; c) S. Ladouceur, E. Zysman-Colman, *Eur. J. Inorg. Chem.* **2013**, 2985-3007; d) Y. You, S. Y. Park, *Dalton Trans.* **2009**, 1267-1282; e) S. Lamansky, P. Djurovich, D. Murphy, F. Abdel-Razzaq, H.E. Lee, C. Adachi, P. E. Burrows, S. R. Forrest, M. E. Thompson *J. Am. Chem. Soc.* **2001**, *123*, 4304-4312.
- [8] a) A. Schaly, Y. Rousselin, J.-C. Chambron, E. Aubert, E. Espinosa, *Eur. J. Inorg. Chem.* **2016**, 832-843; b) J. J. Henkels, C. J. Carruthers, S. E. Chambers, R. Clowes, A. I. Cooper, J. Fisher, M. J. Hardie, *J. Am. Chem. Soc.* **2014**, *136*, 14393-14396; c) Z. Zhong, A. Ikeda, S. Shinkai, S. Sakamoto, K. Yamaguchi, *Org. Lett.* **2001**, *3*, 1085-1087.
- [9] CCDC 1486233 contain the supplementary crystallographic data for this paper. These data are provided free of charge by The Cambridge Crystallographic Data Centre.
- [10] a) C.-T. Wang, L.-C. Shiu, K.-B. Shiu *Chem.-Eur. J.* **2015**, *21*, 7026-7029; b) V. Chandrasekhar, T. Hajra, J. K. Bera, S. M. W. Rahaman, N. Satumtira, O. Elbjeirami, M. A. Omary, *Inorg. Chem.* **2012**, *51*, 1319-1329; c) E. Baranoff, I. Jung, R. Scopelliti, E. Solari, M. Gratzel, Md. K. Nazeeruddin, *Dalton Trans.* **2011**, *40*, 6860-6867; d) W.-S. Sie, G.-H. Lee, K. Y.-D. Tsai, I.-J. Chang, K.-B. Shiu, *J. Mol. Struct.* **2008**, *890*, 198-202.
- [11] While NMR spectra of (\pm)-L1 remain unchanged with time, small additional peaks appear in the ^1H NMR spectra of CD_3NO_2 -solutions of resolved L1 at room temperature (Fig. S2). This may be due to an unknown minor decomposition or saddle-like conformation from crown-saddle-crown racemisation, see for example G. Huber, T. Brotin, L. Dubois, H. Desvaux, J.-P. Dutasta, P. Berthault, *J. Am. Chem. Soc.* **2006**, *128*, 6239-6246.

- [12] J. J. Henkelis, J. Fisher, S. L. Warriner, M. J. Hardie, *Chem. -Eur. J.* **2014**, *20*, 4117-4125.
- [13] a) P. Bonakdarzadeh, F. Pan, E. Kalenius, O. Jurček, K. Rissanen, *Angew. Chem. Int. Ed.* **2015**, *54*, 1480-14893; b) D. L. Caulder, R. E. Powers, T. N. Parac, K. N. Raymond, *Angew. Chem. Int. Ed.* **1998**, *37*, 1840-1843. c) J. L. Bolliger, A. M. Belenguer, J. R. Nitschke, *Angew. Chem. Int. Ed.* **2013**, *52*, 7958-7962; d) T. Liu, Y. Liu, W. Xuan, Y. Cui, *Angew. Chem. Int. Ed.* **2010**, *49*, 4121-4124; e) S. P. Argent, T. Riis-Johannessen, J. C. Jeffery, L. P. Harding, M. D. Ward, *Chem. Commun.* **2005**, 4647-4649.
- [14] a) S. A. Boer, D. R. Turner, *Chem. Commun.* **2015**, *51*, 17375-17378; b) L.-L. Yan, C.-H. Tan, G.-L. Zhang, L.-P. Zhou, J.-C. Bünzli, Q.-F. Sun, *J. Am. Chem. Soc.* **2015**, *137*, 8550-8555; c) C. Gütz, R. Hovorka, G. Schnakenburg, A. Lützen, *Chem. Eur. J.* **2013**, *19*, 10890-10894; d) C. Maeda, T. Kamada, A. Osuka, *Chem. Soc. Rev.* **2007**, *251*, 2743-2752.
- [15] E. Baranoff, E. Orselli, L. Allouche, D. Di Censo, R. Scopelliti, M. Grätzel, M. K. Nazeeruddin, *Chem. Commun.* **2011**, *47*, 2799-2801.

Entry for the Table of Contents (Please choose one layout)

Layout 2:

COMMUNICATION

Victoria E. Pritchard, Diego Rota Martir,
Samuel Oldknow, Shumpei Kai, Shuichi
Hiraoka, Nikki J. Cookson, Eli Zysman-
Colman*, Michaele J. Hardie*

Page No. – Page No.

**Homochiral self-sorted and emissive
Ir(III) metallo-cryptophanes**

Homochiral $[\{\text{Ir}(\text{ppy})_2\}_3(\text{L})_2]^{3+}$ metallo-cages are obtained from the assembly of $(\Lambda, \Delta)\text{-}[\text{Ir}(\text{ppy})_2(\text{MeCN})_2]^+$ with racemic cavitand host molecules decorated with pyridyl-ligands (L), and ligand-exchange is observed in solution. Cages are emissive, and small differences in the L-ligands lead to quite distinct emission properties. Ppy = 2-phenylpyridinato.

